ELSEVIER

Journal of Chromatography A, 786 (1997) 209–218

JOURNAL OF CHROMATOGRAPHY A

Gel permeation chromatography of polymers degrading randomly in the column
Theoretical treatment and practical aspects

Zdeněk Kabátek, Bohuslav Gaš, Jiří Vohlídal*

Department of Physical and Macromolecular Chemistry, Faculty of Science, Charles University, Albertov 2030, 128 40 Prague 2, Czech Republic

Received 24 February 1997; received in revised form 23 May 1997; accepted 23 May 1997

Abstract

Gel permeation chromatography (GPC) separation accompanied with the random degradation of polymer in the column is modelled by a set of continuity equations. Numerical solution of the equations yields: (i) time evolution of the axial concentration profiles of all X-mers that visualize a course of the processes running in the column; and (ii) the number-distribution function of degrees of polymerization (DP) of each polymer fraction passing through the detector (i.e., of each GPC-slice). These data are evaluated by the exact approach way and by conventional methods based on DP values taken from the calibration curve or measured by a light-scattering (LS) detector. Thus obtained DP averages are compared with each other, with those predicted by the theory of polymer random degradation and with those of the non-degraded original polymer. The procedure of determination of the degradation rate constant and original values of DP averages of the degrading polymer with a help of the kinetic equation of random degradation has been also simulated and the following conclusions have been reached: the degradation rate constant is available from GPC measurements performed with the use of both a single concentration detector and its combination with the LS detector. In contrast, the values of DP averages of original non-degraded polymer are not available except for the original weight-average DP provided that values of weight-average DP of degraded polymer are measured with an LS detector. Extrapolation to zero degradation time of the DP values obtained by the calibration curve method yields overestimated DP values of non-degraded polymer. © 1997 Elsevier Science B.V.

Keywords: Size-exclusion chromatography; Degradation kinetics; Rate constants; Polymers

1. Introduction

Gel permeation chromatography (GPC), often referred to as size-exclusion chromatography (SEC), is perhaps the most widely used method for the molecular-mass characterization of polymers. Therefore, it has been subjected to many experimental and theoretical studies concerning almost all possible phenomena interfering with the main, size-exclusion-based partition of macromolecules: (i) axial dispersion consisting of the molecular and eddy diffusion [1–8]; (ii) thermodynamically controlled partition based on the adsorption and/or association equilibria including macromolecules under analysis [1,2,5,7–15]; (iii) reptation of macromolecules in the gel pores [1,2,11,16–18]; (iv) non-destructive hydro-

*Corresponding author.

0021-9673/97/$17.00
PII S0021-9673(97)00604-3

dynamic effects of the flow field [2,9,11] and (v) degradation of long chains in the domains of the extensional flow [1,2,5,19]. Another process that in some cases can interfere with the size-exclusion-based fractionation is a chemical degradation of the polymer under analysis inside the GPC column. This is actual, e.g., in the case of hydrolytically unstable polymers in aqueous eluents (like cellulose in cadoxene) and, perhaps more evidently, in the case of oxygen-sensitive polymers, like polymers of substituted acetylene [20].

The substituted acetylene polymers are known to undergo a rapid autooxidative degradation when exposed to air even in mild conditions at room temperature [21–27]. For example, poly(phenylacetylene) (PPhA) degrades autoxidatively when exposed to air [22–25] obeying the kinetic laws characteristic of the random degradation of polymers [27–32]. The rate constant of degradation, ν, was found to be $2.5 \cdot 10^{-6}$ min^{-1} for PPhA dissolved in tetrahydrofuran (THF; typical eluent in SEC) but ca. hundred times lower ($2 \cdot 10^{-8}$ min^{-1}) for the solid PPhA [25].

From the value of the degradation rate constant, ν, the mean lifetime τ of a macromolecule with the degree of polymerization (DP) X can be easily calculated using the formula: $\tau = 1/(\nu X)$. In case of PPhA macromolecules with $X = 4000$ dissolved in THF, the value of τ is equal to 100 min. Within this time period, only 43.4% of the original macromolecules of this length remain intact, with the remainder being cleaved into fragments. Consequently, the distributions and averages of X of the injected and eluted polymer samples can differ significantly provided that the polymer autooxidative degradation takes also place inside GPC columns. Recently, this suspicion was confirmed experimentally [20].

The subject of the present paper is the general mathematical description of the GPC analysis of a polymer which degrades randomly in the column and the numerical solution to the derived differential equations. The main goals are: (i) to obtain a detailed insight into the overall process running inside the GPC column; (ii) to estimate errors in the distributions and averages of DP obtained by conventional methods of evaluation of GPC records with the help of the calibration curve or DP values measured by a light-scattering (LS) detector; and (iii) to inspect the reliability of experimental values of the degradation rate constant ν and the original DP averages of non-degraded polymer.

2. Theory

GPC on porous systems always comprises two processes, at least: the size-exclusion-based separation and the axial dispersion of macromolecules under analysis [1,2,11]. In our model, these two principle processes are completed with the random degradation of macromolecules under analysis. The following assumptions have been made:

(a) The GPC separation proceeds in the mixed-bed type column such that the separation efficiency for any X-mer does not vary along the column axis.

(b) The column calibration dependence, log X vs. t_X, where t_X is the elution time of a macromolecule with DP equal to X, is linear throughout the whole range of values X taken into account: $\log X = A - Bt_X$, where A and B are the calibration constants for a given column and a polymer–solvent system. This assumption is not unconditionally needed in the model, however, it is practically fulfilled in the case of mixed-bed columns of good quality;

(c) The randomly degrading polymer is linear and neither branching nor cyclization of original macromolecules and/or their fragments takes place during the GPC analysis such that the relation between hydrodynamic dimensions and DP is the same for all macromolecules in the system under consideration.

The result of size-exclusion-based partitioning of a polymer in a GPC column is that the macromolecules with a given DP value of X move along the column axis with an explicit average velocity, v_X. Values of v_X, can be calculated from the calibration dependence and the distance of detector from the column input, L:

$$v_X = \frac{L}{t_X} = \frac{LB}{A - \log X} \tag{1}$$

The kinetics of polymer degradation is generally described by the Simha–Montroll equation [28,29] which indicates how the number of polymer chains of DP equal to X, N_X, varies with the time of degradation, t. In the case of randomly degrading

polymer, i.e., if each of $(X-1)$ main-chain bonds of any macromolecule is equally accessible to scission, the Simha–Montroll equation can be written as:

$$\frac{dN_X}{dt} = -(X-1)\nu N_X + 2\nu \sum_{S=X+1}^{\infty} N_S, \quad X = 1, 2, 3,... \tag{2}$$

where ν is the rate constant of a main-chain bond cleavage, i.e., the probability that a randomly selected bond will cleave within a unit time interval. The first term in Eq. (2) represents the rate of decay of X-mer macromolecules and the second term the rate of their formation in degradation of macromolecules with DP equal to $S>X$. The coefficient 2 in the second term describes the fact that the X-mer can be obtained from a particular S-mer by two kinetically equivalent ways: by disruptions at the distances X and $S-X$ from the same end of the macromolecule. After dividing Eq. (2) by the Avogadro constant and a volume element, numbers of X-mers and S-mers can be replaced by the molar concentrations c_X and c_S.

Inside the GPC column the concentrations must be considered as a function of both the time of analysis t, $t \geq 0$ (that is identical to the time of degradation here) and the column axial coordinate z, $z \in (-\infty,\infty)$, so that $c_X = c_X(z,t)$. The process of GPC fractionation of the degrading polymer can be then described by the following set of continuity equations:

$$\frac{\partial c_X}{\partial t}(z,t) = D_X \frac{\partial^2 c_X}{\partial z^2}(z,t) - v_X \frac{\partial c_X}{\partial z}(z,t) - (X-1)\nu c_X(z,t) + 2\nu \sum_{S=X+1}^{\infty} c_S(z,t), \quad X = 1, 2, 3,.... \tag{3}$$

where D_X is the axial dispersion coefficient of X-mer molecules. On the right hand side of Eq. (3), the first term describes the axial dispersion effect, the second term (originated from Eq. (1)) the effect of size-exclusion-based partitioning of analysed polymer and the third and fourth terms (originated from Eq. (2)) the effect of the polymer random degradation.

The axial dispersion comprises several contributions, mainly the molecular diffusion and eddy diffusion. It can be supposed in case of macromolecules that an effect of the size-dependent molecular diffusion is negligible as compared to the effect of size-independent eddy diffusion. Therefore, the coefficient D_X can be replaced by the apparent dispersion coefficient D_a postulated to be independent of X.

Initial conditions in the unbounded column needed for a numerical solution of Eq. (3) can be defined as follows.

(a) The initial axial concentration profile of an X-mer, $c_X(z,0)$, at $t=0$ is given by

$$c_X(z,0) = c^0(z) f^0(X) \tag{4}$$

where $f^0(X)$ is the original number distribution function of DP of the injected (original) polymer and the function $c^0(z)$ satisfies the following conditions:

$$c^0(z), \frac{\partial c^0}{\partial z}(z) \to 0 \; for \; |z| \to \infty \tag{5}$$

(b) As the total number of moles (substance amount) of monomeric units in the SEC column, n_U, has to remain constant during the GPC separation process, the function $c_X(z,t)$ will satisfy the condition:

$$P \sum_{X=1}^{\infty} X \int_{-\infty}^{\infty} c_X(z,t)dz = n_U, \quad t \geq 0 \tag{6}$$

where P is a cross-section of the column. As follows from Eqs. (4) and (6), the function $c^0(z)$ has to fulfil the condition

$$\int_{-\infty}^{\infty} c^0(z)dz = \frac{n_U}{P < X >_n^0} \tag{7}$$

Here $< X >_n^0$ is the number-average DP of original non-degraded polymer.

3. Computations

The set of partial differential equations (Eq. (3)) was solved numerically and the obtained data were evaluated using the input parameters and methods stated below.

3.1. Input parameters

(a) The following values of the rate constant of

polymer random degradation were chosen: $\nu=0\ s^{-1}$ (the reference computation for non-degrading polymer); $\nu=4\cdot10^{-8}\ s^{-1}$ (the value typical of the degradation of PPhA and its derivatives in solution [20,25,33]); $\nu=4\cdot10^{-7}\ s^{-1}$ (to show the effect of polymer degradation more profoundly).

(b) The value of the apparent dispersion coefficient, D_a, was set to $6\cdot10^{-9}\ m^2\ s^{-1}$. This value was determined experimentally for phenylacetylene in the PL-gel mixed-bed-C column (Polymer Labs., Bristol, UK) from the elution peak dispersion, σ^2, using the Einstein relation: $\sigma^2=2D_at$.

(c) The Gauss function:

$$c^0(z)=C^0\exp\left(-\frac{(z-z_0)^2}{2\sigma^2}\right) \quad (8)$$

with $z_0=0.0075$ m, $\sigma=0.00125$ m and $C^0=1.15\cdot10^{-4}$ mol m^{-3} was considered as the initial profile of the injected polymer sample $c^0(z)$.

(d) The initial number distribution of DP of injected polymer, $f^0(X)$, was supposed to be of the Schulz–Zimm type [34,35]:

$$f^0(X)=\frac{a^b}{\Gamma(b)}X^{b-1}\exp(-aX) \quad (9)$$

where Γ is the gamma function,

$$a=\frac{1}{<X>_w^0-<X>_n^0} \quad \text{and}$$

$$b=\frac{<X>_n^0}{<X>_w^0-<X>_n^0}$$

Here $<X>_n^0$ and $<X>_w^0$ are the initial number- and weight-average DP of the polymer, respectively. A polymer with medium narrow distribution, $<X>_w^0=7500$ and $<X>_n^0=5000$, was used in computations.

(e) The calculation was performed on the column of total length of 0.5 m and a hypothetical detector was positioned at the distance of $z_D=(0.3\ m+z_0)$ from the beginning of column (it means that $L=0.3$ m). The average velocities of particular X-mers were calculated according to Eq. (1) using the real values of calibration constants $A=12.117$ and $B=0.01885\ s^{-1}$ found for polystyrene in THF and the mixed-bed-C column.

3.2. Computation method

The program for solution of partial differential equations (Eq. (3)) was written in Pascal language and ran on a personal computer with 20 MB RAM. The spatial coordinate was discretized at a set of 800 grid points to generate a set of ordinary differential equations with the time as independent variable. Hammings predictor–corrector method [36] was applied for the solution except for the first four time points for which the Runge–Kutta method was used. The time increment of discretization was set to 0.5 s. The computation was made for 115 discrete values of X: 1, 2, 3, 4, 5, 7, 10, 14, 19... and further approximately linearly in the logarithmic scale up to 30 000. For this maximum value, the condition $\Sigma_{X=1}^{30000}f(X)\rightarrow1$ was fulfilled satisfactorily.

Precision of numerical computation was continuously examined by a verification of constancy of the total number of monomeric units n_U in the system according to Eq. (6). Values of $c_X(z,t)$ for X values not involved in the above series but, needed for this verification, were obtained by the Lagrange interpolation. The maximum loss in n_U caused by numerical errors in computation was found to be 0.007%, 0.05% and 0.34% for calculations performed with values of ν equal to 0 s^{-1}, $4\cdot10^{-8}\ s^{-1}$ and $4\cdot10^{-7}\ s^{-1}$, respectively.

3.3. Data treatment and evaluation

Current values of $c_X(z,t)$ for all chosen X were stored each 100 s and the obtained axial concentration profiles of X-mers were used for visualization of the process of polymer fractionation and degradation in the GPC column (see Section 4).

At axial variable $z=z_D$ (the detector position), the values of t_i and $c_X(z_D,t_i)$ corresponding to the ith GPC-slice (the polymer fraction passing through the detector at time t_i) were continuously collected at every time increment and stored for all values of X and t_i. These data correspond with the number-distribution function of DP of the polymer fraction involved in every ith GPC-slice. These functions were used for calculation of the following ith GPC-slice quantities: (i) $R_w(t_i)=\Sigma\{Xc_X(z_D,t_i)\}$ simulating the record of a weight-concentration detector; (ii) $R_n(t_i)=\Sigma\{c_X(z_D,t_i)\}$ simulating the record of a hypo-

thetical mole-concentration detector; (iii) $R_z(t_i) = \Sigma\{X^2 c_X(z_D,t_i)\}$ simulating the record of a hypothetical z-concentration detector; (iv) weight-average DP, $<X>_{w,i}$, corresponding to the output of an LS detector; (v) number-average DP, $<X>_{n,i}$, and the polydispersity index based on the number-distribution function of DP, $I_{n,i} = <X>_{w,i} / <X>_{n,i}$; and (vi) z-average DP, $<X>_{z,i}$, and the polydispersity index based on the weight-distribution function of DP, $I_{w,i} = <X>_{z,i} / <X>_{w,i}$.

The simulated data have been evaluated by the following methods:

(a) Calibration curve method. Here we intended to simulate the most widely used procedure of evaluation of GPC data obtained with an apparatus with a weight-concentration detector. The method uses $R_w(t_i)$ values and values of X_i taken from the column calibration dependence, considering the GPC-slices as to be monodisperse [1].

(b) LS detector method. This method uses the $R_w(t_i)$ values obtained from a weight-concentration detector and corresponding $<X>_{w,i}$ values obtained from an LS detector [1].

(c) Exact approach. Here the simulated data are evaluated by a theoretically correct way. The couples of conjugated quantities: $R_n(t_i)$ and $<X>_{n,i}$, $R_w(t_i)$ and $<X>_{w,i}$, and $R_z(t_i)$ and $<X>_{z,i}$, are used for a calculation of the respective number-, weight- and z-averages and distribution functions of DP. It should be realized that values of all these quantities are not available at any real GPC equipment such that the exact approach can be applied only on the data obtained by a simulation like in the present model.

4. Results and discussion

4.1. Single GPC analysis of a degrading polymer

The main points of interest to be discussed here are how the mean values and distributions of DP of degrading polymer measured with a use of various detection systems differ: (i) from each other; (ii) from those resulting from the theory of polymer random degradation; and (iii) from those of original (injected) sample.

A simulated process of the GPC fractionation of non-degrading polymer ($\nu = 0$) (i.e., the results of the reference simulation) is shown in Fig. 1a. The separation of X-mers along the column z-axis and broadening of X-mer peaks due to axial dispersion are clearly seen. The values of $<X>_n$ and $<X>_w$ obtained by evaluation of the simulated GPC records by all the above methods are in a good agreement with those used as the input (see Table 1), which testifies to reliability of the used model and computation methods.

The influence of slow but significant polymer degradation ($\nu = 4 \cdot 10^{-8}$ s^{-1}) on the partition process is visualized in Fig. 1b as additional broadening of the lower and medium X-mer peaks (a dark trace at the bottom of diagrams). This broadening of lower X-mer peaks goes down to domains of higher X-mers because molecules involved in these "forward tails" are the fragments of already divided chains of higher X-mers. The effect of polymer degradation is more profoundly demonstrated in Fig. 1c as an the example of the faster degrading polymer ($\nu = 4 \cdot 10^{-7}$ s^{-1}). In this case a majority of the lower and medium X-mers passing through the detector mainly consists of fragments of degraded original macromolecules.

Simulated GPC records $R_w(t_i)$ and time dependence of polydispersity indices $I_{n,i}$ of GPC-slices are shown in Fig. 2. As expected, the higher the rate of polymer degradation, the higher is the polydispersity of GPC-slices. This of course means that the error in evaluation of the $R_w(t_i)$ records by the calibration curve method should rise as the rate of polymer degradation increases. The values of DP averages calculated in this way must be overestimated due to assignment of overestimated values of X_i to all GPC-slices (see Table 1).

The logarithmic number-distribution and weight-distribution functions of DP, $f(\log X)$ and $w(\log X)$, respectively, obtained by various evaluation methods are compared with each other and with those of injected polymer in Fig. 3. The distributions obtained by the exact approach evaluation of simulated data (curve 4) can be regarded as the best approximation of the actual DP distribution at the time corresponding to the GPC record apex, t_{ap}. It should be stressed here that, from the theory point of view, a correct instantaneous distribution of DP of any degrading polymer cannot be obtained by any GPC detector system because the detector responses $R_n(t_i)$ and $R_w(t_i)$ pertaining to ith GPC-slices are not

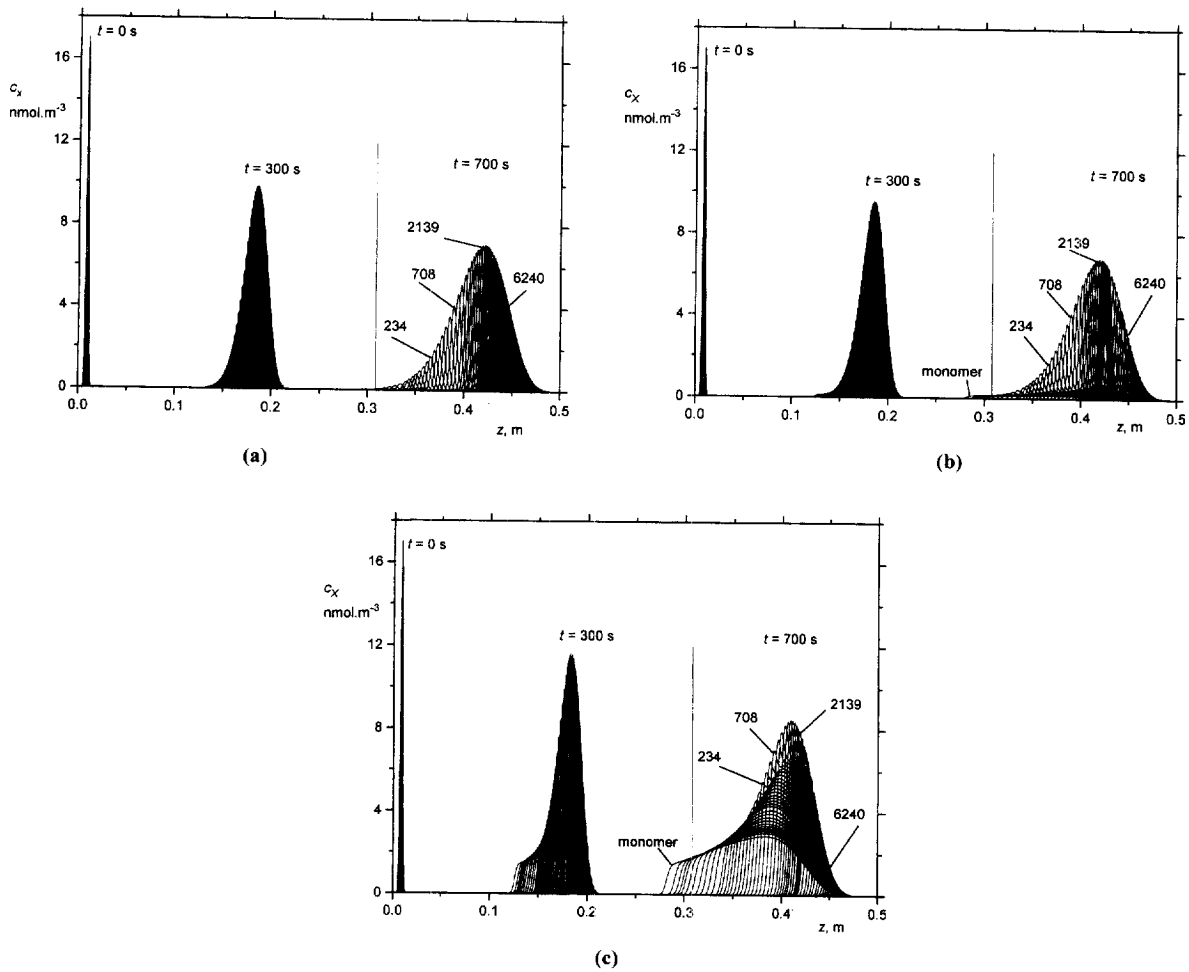

Fig. 1. Simulated axial concentration profiles of selected X-mers at the beginning ($t=0$) and after 300 s and 700 s of the process of GPC separation. Part, value of ν (s^{-1}): (a) 0; (b) $4\cdot10^{-8}$; (c) $4\cdot10^{-7}$. The vertical line at $z=0.3075$ m marks the detector position.

Table 1
Comparison of the values of polymer characteristics obtained by various evaluation methods

	ν (s^{-1})	Calibration curve	LS detection	Exact approach	Eqs. (10) and (11)
$<X>_n$	0	4978	5086	4997	5000
$<X>_n$	$4\cdot10^{-8}$	4800	4756	4548	4568
$<X>_n$	$4\cdot10^{-7}$	3643	3000	2540	2543
$<X>_w$	0	7508	7491	7491	7500
$<X>_w$	$4\cdot10^{-8}$	7335	7050	7050	7052
$<X>_w$	$4\cdot10^{-7}$	5646	4541	4541	4501
$<I>_n$	0	1.51	1.47	1.50	1.50
$<I>_n$	$4\cdot10^{-8}$	1.53	1.48	1.55	1.54
$<I>_n$	$4\cdot10^{-7}$	1.55	1.51	1.78	1.77

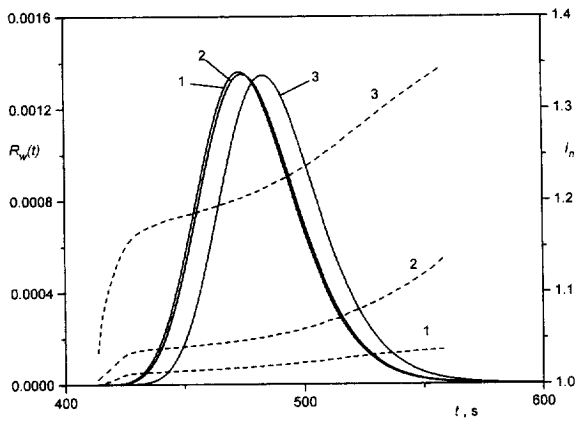

Fig. 2. Simulated records of a weight-concentration detector $R_w(t)$ (solid lines) and the polydipersity indices of GPC-slices $I_{n,i} = <X>_{w,i}/<X>_{n,i}$ (dashed lines). Curve, value of ν (s^{-1}): (1) 0; (2) $4\cdot10^{-8}$; (3) $4\cdot10^{-7}$.

collected in one moment. The time period of scanning the GPC records commonly overreaches 150 s (see Fig. 2) and during this period a significant change in the DP distribution of degrading polymer can come into being.

As shown in Fig. 3, the relative deviation from the correct DP distributions (represented by curves 4) is always higher for $f(\log X)$ than for $w(\log X)$. The weight-distribution function $w(\log X)$ obtained by

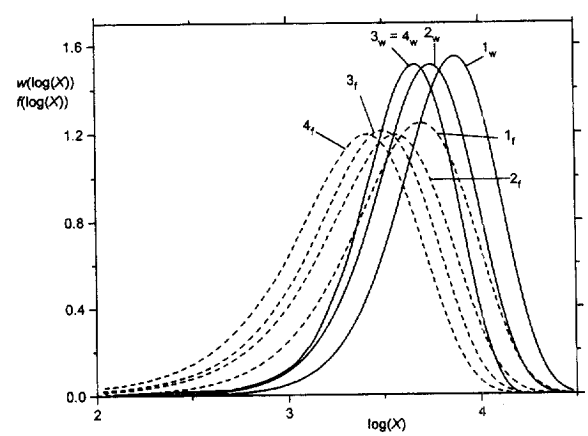

Fig. 3. Comparison of the logarithmic distribution functions of DP of non-degraded polymer (curve 1) with those obtained by evaluation of the simulated GPC records by: calibration curve method (2); LS detector method (3) and exact approach method (4). Subscript n denotes the number-distributions, $f(\log X)$ and subscript f the weight-distributions, $w(\log X)$.

the LS detector method is identical to that obtained by the exact approach method because both are calculated from the same data by the same formula. On the contrary, the polymer number-distribution function $f(\log X)$ acquired by the LS detector method (curve 3_f) is shifted towards higher values of X due to the use of available values of $<X>_{w,i}$ instead of values of $<X>_{n,i}$ which should be applied in correct calculation. The distributions, $f(\log X)$ and $w(\log X)$ obtained with a use of the calibration curve method are both shifted towards higher values of X due to analogous reasons: the value of X_i assigned to a particular ith GPC-slice is always higher than those which should have been correctly used, the overestimation being higher for $<X>_{n,i}$ than for $<X>_{w,i}$.

Values of $<X>_n$, $<X>_w$ and I_n obtained by particular evaluation methods are summarized in Table 1 in which also the values calculated from Eqs. (10) and (11) describing the kinetics of the polymer random degradation [28,29,32] are included for a comparison.

$$\frac{1}{<X>_n^t} = \frac{1}{<X>_n^0} + \nu t \tag{10}$$

$$\frac{1}{<X>_w^t} = \frac{1}{<X>_w^0} + \frac{\nu}{3}\int_0^t I_w(t)\mathrm{d}t \tag{11}$$

Here $<X>_n^0 = 5000$ and $<X>_w^0 = 7500$ are the corresponding averages of DP of the originally injected polymer at time $t=0$ and $I_w(t) = <X>_z^t / <X>_w^t$ is the polydispersity index based on the polymer weight-distribution of X at the degradation time t. The time of the $R_w(t_i)$ record apex, $t = t_{ap}$, was used in calculations according to Eqs. (10) and (11). The integral on the right hand side of Eq. (11) was obtained by the numerical integration based on the values of I_w calculated in the course of simulation.

As in Table 1, the values of DP averages and polydispersity indices obtained by the exact approach evaluation of simulated data are almost identical with those calculated from the kinetic Eqs. (10) and (11). The observed small differences are due to numerical errors of computation. The $<X>_w$ values obtained by the LS detector method are also correct, of course. In contrast, the $<X>_n$ values obtained by the LS detector method are always overestimated

(even in case of non-degrading polymer) which is due to a use of $<X>_{w,i}$ values (instead of $<X>_{n,i}$ values) in the calculation of $<X>_n$ (intrinsic error of this method). Consequently, the LS detector polydispersity indices I_n are underestimated.

Perhaps most notable is the fact that in the case of degrading polymers the values of both $<X>_n$ and $<X>_w$ obtained by the calibration curve method are significantly overestimated, the relative increase being more pronounced at higher values of the rate constant ν. The axial concentration profiles shown in Fig. 1b,c visually document the above-mentioned explanation. It is evident that the GPC-slices of higher X-mers comprise various low-DP fragments which contribute to the detector response $R_{w,i}$. However, a value X_i assigned to ith GPC-slice from the calibration curve belongs to the largest included (i.e., yet non-degraded original) molecules regardless the presence of smaller fragments. There is no other possibility here. Due to this systematic error of the evaluation method both $<X>_n$ and $<X>_w$ values have to be overestimated.

4.2. Estimation of the degradation rate constant and the DP characteristics of non-degraded polymer

It is evident that the original values of $<X>_n^0$ and $<X>_w^0$ of non-degraded polymer are not accessible from any single GPC analysis. On the other hand, it was shown in case of PPhA that the rates of polymer degradation in air and in GPC column are approximately the same [20]. Thus the values of $<X>_n^0$ and $<X>_w^0$ might potentially be estimated by extrapolation of $1/<X>_n^t$ vs. t and $1/<X>_w^t$ vs. $\int I_w dt$ dependencies to zero degradation time t (see Eqs. (10) and (11)). For this purpose, a series of consecutive GPC analyses of the same polymer solution is needed.

Practicability of the outlined method has been examined by the simulation of the proposed procedure. The calculated distribution of the polymer (with $\nu = 4 \cdot 10^{-7}\ s^{-1}$) after 700 s of degradation was used as the input into the next computation modelling the first consecutive GPC analysis of the same polymer solution. The obtained GPC records were evaluated and the new distribution after 700 s (i.e., 1400 s in total) was used again as the input in modelling further GPC analysis, etc. The degradation time needed for evaluation of the results fulfils the formula: $t = t_{ap} + 700J$ (in seconds) where $J = 0, 1, 2,...$ denotes the serial number of particular consecutive analysis. Evaluation of thus obtained values of $<X>_n^t$ and $<X>_w^t$ according to Eqs. (10) and (11) is shown in Fig. 4. The extrapolated values of $<X>_n^0$ and $<X>_w^0$ and values of the rate constant ν calculated from the slopes of particular dependence are summarized in Table 2.

The values of $<X>_n^0$, $<X>_w^0$ and ν obtained from the simulation by using the exact approach method data are almost identical with those used as the input which proves to applicability of the performed overall simulation. Time dependence of $<X>_w^t$ values obtained by the LS detector method also yields reasonable values of $<X>_w^0$ but somewhat overestimated values of ν. The increase in ν value is caused by systematic underestimating the values of I_w (see Eq. (11)) which is typical of the conventional LS detector data evaluation (the reason is calculation of the overall value of $<X>_z$ using the $<X>_{w,i}$ instead of correct $<X>_{z,i}$ values pertaining to ith GPC-slice). Due to analog reasons,

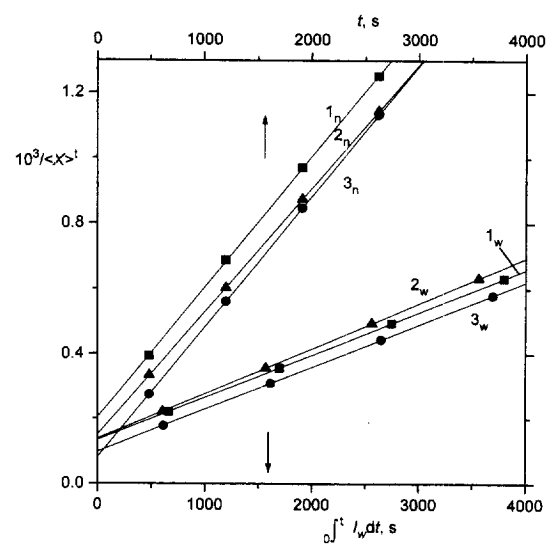

Fig. 4. Evaluation of DP averages $<X>^t$ from simulations of consecutive GPC analyses according to Eqs. (10) and (11). Values of $<X>^t$ obtained by the evaluation of simulated data by: exact approach method (1); LS-detector method (2); calibration curve method (3). Subscript n denotes the number averages and subscript w the weight averages.

Table 2
Values of DP averages and rate constants of degradation obtained from extrapolations according to Eqs. (10) and (11)

	Calibration curve	LS detection	Exact approach	Eqs. (10) and (11)
$<X>_n^0$	12 280	6560	5000	5000
$\nu_n \cdot 10^7$ (s^{-1})	4.01	3.75	4.02	4.00
$<X>_w^0$	10 250	7330	7540	7500
$\nu_w \cdot 10^7$ (s^{-1})	3.95	4.21	3.95	4.00
I_n	0.83	1.12	1.51	1.50

the $<X>_n^t$ values gained by the LS detector method offer significantly overestimated values of $<X>_n^0$ but underestimated values of ν. However, the average of the two values of ν obtained by the LS detector method, $\nu=(\nu_n+\nu_w)/2=3.98\cdot10^{-7}$ s^{-1}, agrees well with the correct value of $\nu=4\cdot10^{-7}$ s^{-1}. A mutual compensation of systematic errors can be suggested as a reason of this result.

As in Table 2, the treatment of $<X>_n^t$ and $<X>_w^t$ values obtained by the calibration curve method (weight-concentration detector) provides incorrect, significantly overestimated values of both $<X>_n^0$ and $<X>_w^0$. This is due to systematic overestimation of all values $<X>_n^t$ and $<X>_w^t$ evaluated according to Eqs. (10) and (11). The most surprising finding is that the extrapolated value of $<X>_n^0$ can be even higher than that of $<X>_w^0$. This can be understood with the help of Fig. 4 taking into account that the absolute difference between reciprocal values of DP obtained by the exact approach method (lines 1_n and 1_w) and calibration curve method (lines 3_n and 3_w) is much higher for $<X>_n^t$ than for $<X>_w^t$ values. There is probably no way of eliminating this systematic error here. On the contrary, the values of rate constant ν obtained from these both type dependence are practically correct. It means that values of ν that have been experimentally determined using the concentration detector data and calibration curve method [21,26,34] can be regarded as reliable.

5. Conclusions

Summarizing the above discussion, the following conclusions of theoretical and practical importance can be drawn.

(1) Significant degradation taking place inside the GPC column can lower the DP of a polymer under analysis to such an extent that the values of DP averages of original (injected), non-degraded polymer are not available from a single GPC measurement. (However, in case of polymers undergoing the oxidative degradation, the original DP averages are in principal available from a single GPC analyses carried out under an inert atmosphere, see Ref. [20]).

(2) The polymer degradation in the column increases the polydispersity of GPC-slices which unavoidably brings systematic errors into the evaluation of GPC records by conventional methods. On account of these errors, the original DP averages and those predicted by the theory of random degradation and determined with a use of conventional evaluation methods can be sentenced into the following sequences: $<X>_n^t$: exact approach$<$LS detector$<$ calibration curve$<$original and $<X>_w^t$: exact approach$=$LS detector$<$calibration curve$<$original.

(3) As far as true values of the DP averages of original, non-degraded polymer are concerned, only the value of $<X>_w^0$ is experimentally available by means of Eq. (11) provided that a series of $<X>_w^t$ values determined by the LS detector method is at ones disposal. The value of $<X>_n^0$ obtained by the LS detector method is always overestimated but fairly not so much as that obtained by the calibration curve method. Values of $<X>_n^0$ and $<X>_w^0$ determined with a use of the calibration curve method can be both overestimated to a great extent. The error introduced due to fact that the condition of monodispersity of GPC-slices is not fulfilled can even result in such incorrect findings that the obtained value of $<X>_n^0$ is higher than that of $<X>_w^0$ and the polydispersity index I_n is lower than 1. It can be thus concluded that a use of the calibration curve

method for a determination of values of $<X>_n^0$ and $<X>_w^0$ should be avoided.

(4) Unlike the preceding case, a reasonably correct value of the degradation rate constant ν can be determined with a use of $<X>_n'$ and/or $<X>_w'$ values obtained by both the calibration curve and the LS detector method.

Acknowledgements

Financial support of the Grant Agency of the Czech Republic (contract Nos. 203/93/2458 and 203/94/0698) and the Commission of EC (PECO program, supplementary contract ERBCIPDCT-940617) is greatly acknowledged.

References

[1] B.J. Hunt and S.R. Holding, Size Exclusion Chromatography, Blackie, Glasgow, 1989.
[2] J.C. Giddings, Unified Separation Science, Wiley, New York, 1991.
[3] L.H. Tung, J.C. Moore, G.W. Knight, J. Appl. Polym. Sci. 10 (1966) 637.
[4] L. Marais, Z. Grubušic-Gallot, H. Benoit, J. Appl. Polym. Sci. 21 (1976) 428.
[5] J. Klein, M. Grtneberg, Macromolecules 14 (1981) 1411–1419.
[6] M. Netopilík, G. Schulz, Acta Polym. 35 (1984) 140.
[7] J. Janča (Editor), Steric Exclusion Liquid Chromatography of Polymers (Chromatographic Science Series, Vol. 25) Marcel Dekker, New York. 1984.
[8] G. Glockner, Polymer Characterization by Liquid Chromatography, (Journal of Chromatography Library, Vol. 34), Elsevier, Amsterdam, 1988.
[9] J.V. Dawkins, Pure Appl. Chem. 51 (1979) 1473.
[10] G. Glockner, Gradient HPLC of Copolymers and Chromatographic Cross-Fractionation, Springer Verlag, Berlin, 1991.
[11] R. Tijssen and J. Bos, in F. Dondi and G. Guiochon (Editors), Theoretical Advancement in Chromatography and Related Separation Techniques, Kluwer Academic Publishers, 1992, p. 397.
[12] K. Procházka, T. Mandák, M. Kočiřík, B. Bednář, Z. Tuzar, J. Chem. Soc. Faraday Trans. 89 (1990) 1103.
[13] K. Procházka, T. Mandák, B. Bednář, J. Trněná, Z. Tuzar, J. Liq. Chromatogr. 13 (1990) 1765.
[14] J. Sedláček, Z. Grubisic-Gallot, Y. Gallot, Macromol. Chem Phys. 195 (1994) 781.
[15] Z. Grubisic-Gallot, Y. Gallot, J. Sedláček, J. Liq. Chromatogr. 18 (1995) 2291.
[16] P. De Gennes, Scaling Concepts in Polymer Physics, Cornell University Press, Ithaca, NY, 2nd ed., 1985.
[17] G. Guillot, L. Leger, F. Rondelez, Macromolecules 18 (1985) 2531.
[18] F. Brochard-Wyart, E. Raphael, Macromolecules 23 (1990) 2276.
[19] J.J. Kirkland, J. Chromatogr. 125 (1976) 231.
[20] J. Vohlídal, Z. Kabátek, J. Sedláček, M. Pacovská, Z. Grubisic-Gallot, Collect. Czech. Chem. Commun. 61 (1996) 120.
[21] J.C.W. Chien, Polyacetylene—Chemistry, Physics and Material Science, Academic Press, New York, 1984.
[22] E.T. Kang, K.G. Neoh, K.L. Tan, Polym. Deg. Stab. 26 (1989) 21.
[23] J.S. Park, S. Serwon, A. Langer, P. Ehrlich, J. Polym. Sci.: Polym. Chem. 27 (1989) 2651.
[24] J. Sedláček, J. Vohlídal, Z. Grubišic-Gallot, Makromol. Chem. Rapid. Commun. 14 (1993) 51.
[25] J. Vohlídal, D. Rédrová, M. Pacovská, J. Sedláček, Collect. Czech. Chem. Commun. 58 (1993) 2651.
[26] H. Shirakawa, T. Masuda and K. Takeda, in S. Patal (Editor), The Chemistry of Triple Bonded Functional Groups, Supplement C2, Wiley, New York, 1994, Ch. 17.
[27] J. Sedláček, M. Pacovská, J. Vohlídal, Z. Grubišic-Gallot, M. Žigon, Macromol. Chem. Phys. 196 (1995) 1705.
[28] R. Simha, Appl. Phys. 12 (1941) 569.
[29] E.W. Montroll, J. Am. Chem. Soc. 63 (1941) 1215.
[30] E.W. Montroll, R. Simha, J. Chem. Phys. 8 (1940) 721.
[31] M. Ballauf, B.A. Wolf, Macromolecules 14 (1981) 654.
[32] J. Vohlídal, Macromol. Rapid Commun. 15 (1994) 765.
[33] J. Vohlídal, J. Sedláček, M. Pacovská, O. Lavastre, P.H. Dixneuf, H. Balcar, J. Pfleger, Polymer 38 (1997) 3359.
[34] G.W. Schulz, Z. Physik. Chem. B34 (1939) 25.
[35] B.H. Zimm, J. Chem. Phys. 16 (1948) 1099.
[36] A. Ralston, First Course in Numerical Methods, McGraw-Hill, New York, 1965.